Applied Physics Letters

RESEARCH ARTICLE | MARCH 12 2024

Continuous variable quantum teleportation network with star topology

Yimiao Wu; Long Tian; Wenxiu Yao; Shaoping Shi; Xuan Liu; Bo Lu; Yajun Wang; Yaohui Zheng

Appl. Phys. Lett. 124, 114002 (2024)
https://doi.org/10.1063/5.0191643

Continuous variable quantum teleportation network with star topology

Cite as: Appl. Phys. Lett. **124**, 114002 (2024); doi: 10.1063/5.0191643
Submitted: 15 December 2023 · Accepted: 1 March 2024 ·
Published Online: 12 March 2024

View Online Export Citation CrossMark

Yimiao Wu,[1] Long Tian,[1,2] Wenxiu Yao,[1] Shaoping Shi,[1,a)] Xuan Liu,[1] Bo Lu,[1] Yajun Wang,[1,2] and Yaohui Zheng[1,2,a)]

AFFILIATIONS

[1]State Key Laboratory of Quantum Optics and Quantum Optics Devices, Institute of Opto-Electronics, Shanxi University, Taiyuan 030006, China
[2]Collaborative Innovation Center of Extreme Optics, Shanxi University, Taiyuan 030006, China

[a)]Authors to whom correspondence should be addressed: ssp4208@sxu.edu.cn and yhzheng@sxu.edu.cn

ABSTRACT

Quantum network allows communication among more than two users with quantum teleportation and high quantum fidelity enabled by non-classical resources. As one of the most versatile architectures, all users are connected mediated by the central station in the star topology network, leading to the realization of the information interconnection and interoperability. In this work, we experimentally demonstrate a 4-branch continuous variable (CV) quantum teleportation network with star topology by employing entangled sideband modes from one squeezed state of light. Here, multiple pairs of entangled sideband modes are distributed on demand to central station and four nodes, respectively. Each node linked to the network has its own communication channel with the central station, where the deterministic CV quantum teleportation protocol is implemented with the fidelities above 0.830.

With the development of quantum information processing, continuous variable (CV) quantum communication protocol, such as quantum teleportation,[1–3] quantum dense coding,[4–7] quantum key distribution,[8–10] and quantum sharing,[11–13] has been discovered and rapidly developed over two decades. Quantum teleportation allows to transfer an unknown state from a sender to a distant receiver with shared quantum entanglement and classical communication.[1,14–20] As the most fundamental Gaussian operation, quantum teleportation represents a basic ingredient in the development of many advanced quantum technologies, including entanglement swapping,[19,21] quantum repeaters,[22] quantum gate teleportation,[23] and quantum computing.[24–26] After implementing the experimental demonstration of quantum teleportation with high fidelity,[27] another focus is the extension of the node number from two users to multi-users, aiming at laying a solid foundation of quantum internet.

To construct a real-world quantum network, it is essential to address the limitations of the security and functionality that results from the extension process.[28,29] Several typical network topologies[30] include the linear topology,[26] ring topology,[31] star graph topology,[32–35] diamond graph topology,[30] fully connected topology,[28,36,37] complex topology that combines multiple simple architectures,[38] etc., with which quantum protocols have been proposed, even experimentally demonstrated. However, there has been far less activity in the development of CV quantum network, compared with discrete variable substrate.[39–44] The CV quantum system operates in infinite dimensional Hilbert space and can be measured through unconditional operations, thereby achieving ultrahigh information transfer rate, which represents an important complement to quantum information processing. Therefore, it is our common pursuit of demonstrating quantum network protocol with CV in virtue of diverse network topology. Currently, the distribution of multiplexed CV entanglement was implemented by the employment of star network topology.[33] However, until now, quantum teleportation protocol has not been demonstrated with star network topology.

Here, we experimentally demonstrate a CV quantum teleportation network with star topology by employing an entanglement optical frequency comb (OFC) from one squeezed light source.[45] To perform the management of entangled sideband modes without coherent amplitude, we construct frequency-comb-type auxiliary control beam with two waveguide amplitude modulators (WGAMs), which gives a nice performance boost for the control loop in the downstream experiment. All of the upper sidebands from squeezed light are distributed to the central station, and each lower sideband is transmitted to each node. Each node linked to the network has its own communication link with the central station at the same time, named as the star topology network. In virtue of shared entanglement states between the central state and each node, quantum teleportation protocols along each quantum link are implemented, with the fidelity of above 0.830. The quantum teleportation network has great potential to scale to more nodes in combination with other network topology and innovative technology.

A tailor-made $n=4$ branch quantum teleportation star network[32–35] is proposed, as illustrated in Fig. 1. The quantum teleportation process is shown in Fig. 1(a). The sideband entanglement modes are distributed to Alice and Bob terminal. In Alice, one-half of the Einstein–Podolsky–Rosen (EPR+) entanglement is combined with the unknown state at a balanced beam splitter (BS). Alice's station consists of Bell-type detection to acquire the amplitude and phase quadrature components of the unknown input state and convert to the electric field. Classical channels are used to transmit Alice's detection results to Bob. The other half of the entangled state (EPR−) held by Bob is transformed with the received measurement results and further reconstructed the complete information of the input state.[3,4] A squeezed field involves a lot of EPR entangled modes at these sidebands within the phase-matching bandwidth of nonlinear crystal and the frequency separation between two adjacent modes is a free spectral range (FSR) of optical parameter oscillator (OPO).[46,47] Thus, we can build a star topology network utilizing the EPR entangled sideband modes. The central station possesses all upper sidebands; meanwhile, lower sidebands are allocated each node, as shown in Fig. 1(b). Each node linked to the network has its own communication link with the central station at the same time; the quantum teleportation between the central station and any node can be implemented utilizing shared entanglement states. As the information sender, the central station can transfer an unknown input state to any node, vice versa. The number of nodes, denoted by n, is determined by the prepared entangled sideband modes.

As a basic resource of constructing quantum star network, it requires that the entangled sideband modes have the features of compactness, robustness, and ease of operation.[3,4,48] In our previous works, a frequency-comb-type control beam that is generated from two waveguide phase modulators (WGPMs) is phase locked to the carrier of squeezed light to manage the cavities and relative phases in the downstream experiment.[49] However, the additional phase locking loop inevitably induces additional loss. To avoid the loss, we utilize a frequency-comb-type beam as the seed beam of the OPO,[50] which serves as the control beam with coherent amplitude. Unfortunately, there is a contradiction between the generation of high-order sideband modes and the error signal with high signal-to-noise ratio (SNR), which confines the controlled maximum order number to two.[50] In order to overcome the limitation, we expect to find an innovative technology for the extension of the controlled sideband number. Amplitude modulator (AM) that represents a significant candidate is also used to generate frequency-comb-type beam.

The structures of WGPM and WGAM are shown in Fig. 2(a). When seed beam with frequency-comb-type structure is directly injected in OPO, all of its frequency components determine the amplitude of the error signal for squeezed angle manipulation. The squeezed angle is a very important parameter of squeezed state generation, which should be carefully stabilized to the most deamplified phase or the amplified phase.[51,52] By utilizing the photo detector (PD1) to extract the error signal, we use the Pound–Drever–Hall (PDH) technique to control the squeezed angle, as depicted in Fig. 2(b). The ring filter cavity (RFC) as a frequency dependence beam splitter is used to observe each sideband mode status (amplification or deamplification). In this case of phase modulator (PM), as shown in Fig. 2(c), the odd and even-order sideband modes have an opposite parametric process due to their different phase: one is for the parametric amplification process, another is for the parametric deamplification one. For the amplitude modulator case, all sideband modes have the same phase with the carrier, which presents the same parametric process, shown in Fig. 2(d).[49]

In the two cases of generating the frequency-comb-type seed beam (FCSB) by the employment of WGPM and WGAM, the SNR of the error signal for squeezed angle manipulation can be expressed as

$$SNR_{PM} = \sum_{j=0}^{\infty} (-1)^j [Bessel(j,m)]^2 * \sin(\varphi/2), \qquad (1)$$

$$SNR_{AM} = \sum_{j=0}^{\infty} [Bessel(j,m)]^2 * \sin(\varphi/2), \qquad (2)$$

where j is the order of the sideband modes, m is the modulation depth, and φ is the squeezed angle, subscript PM (AM) is the case of phase (amplitude) modulator. For the case of WGPM, the SNR of the error signal presents a damped-oscillation-like trend as the modulation depth increase. Especially for the manipulation of high-order sideband

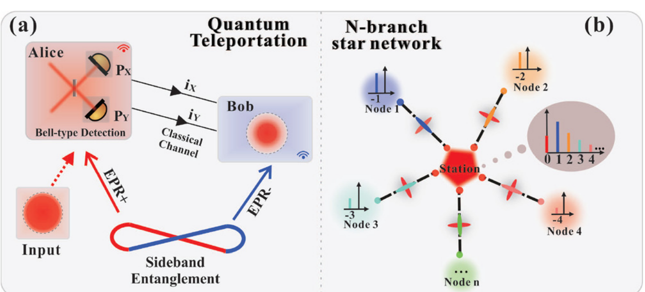

FIG. 1. Schematic diagram of the CV quantum teleportation network with star topology. (a) Quantum teleportation protocol. (b) N-branch star-topology network with optical frequency comb system.

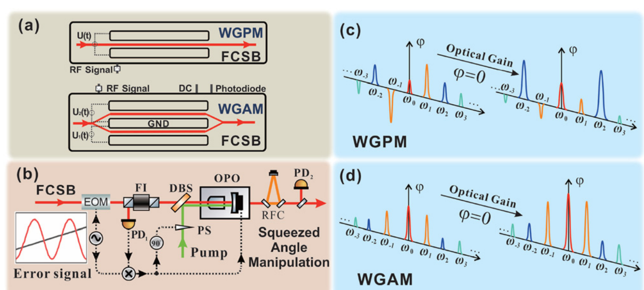

FIG. 2. (a) Structure of the waveguide phase modulator (WGPM) and waveguide amplitude modulator (WGAM). (b) Experimental scheme of manipulating the squeezed angle. (c) and (d) Schematic diagram of each sideband modes status (amplification or deamplification) of WGPM and WGAM.

mode, high modulation depth is needed to generate enough power of the sideband, and the degradation of the error signal is not tolerated. Fortunately, the SNR remains unchanged in the WGAM case, which perfectly addresses these problems that occurs with a WGPM (see more details in the supplementary material).

In Fig. 3(a), utilizing two fiber-coupled WGAMs, we implement a specific FCSB scheme to experimentally demonstrate the quantum teleportation network with star topology (see more details in the supplementary material). The WGAM_1 simultaneously generates sideband modes $\omega_{\pm 1}$, $\omega_{\pm 2}$, $\omega_{\pm 3}$ with a modulation frequency of 3.325 GHz that is equal to the FSR of OPO. The WGAM_2 is used to produce the sideband modes $\omega_{\pm 4}$ with a modulation frequency of 13.3 GHz. Two FCSBs are combined on a 10:90 BS with the relative phase of 0 and then coupled into the OPO. A squeezed field involves many EPR entangled modes at the symmetric sidebands of around the half-pump frequency within the phase-matching bandwidth of the nonlinear crystal, and the squeezed bandwidth is determined by the cavity linewidth of 68 MHz. Each pair of the entangled modes can independently perform the quantum teleportation protocol. The squeezed angle is accurately locked to 0 with pump factor of 0.8 and the classical gain of 30. Four cascade ring filter cavities (RFCs) are used to separate the lower sideband modes $\mathrm{EPR}_{-\omega}$ – $\mathrm{EPR}_{-4\omega}$ that serves as the quantum resource of node n ($n = 1, 2, 3, 4$). All of the upper sideband modes EPR+ are delivered to the central station. The RFCs are the near-impedance matching cavities with the linewidth of 66.0, 63.7, 62.0, and 43.4 MHz, respectively, which could efficiently separate the sideband modes and reduce the decoherence.[51,53] The power of the four entangled single sidebands is 48.6, 12.15, 12.15, and 13.23 μW, respectively. It is enough to actively stabilize and extract the acquired sideband modes. A WGPM with the maximum input power about 300 mW is introduced to generate the local oscillators (LOs), the input state, and auxiliary beam (AUX) with the same frequency as corresponding entangled sideband modes. The LO mode cleaners (MCs) with the linewidth of 2 MHz avoid interfering with the quadrature measurement.[49,50]

The upper sideband modes are coupled with the unknown input state at a balanced BS, and the output fields perform a joint quantum measurement by two balanced homodyne detectors (BHDs) to extract the amplitude (P_X) and phase quadrature (P_Y) information at the central station, respectively, as shown in Fig. 3(b). After adjusting the classical gain (g_X, g_Y), the detected signals are transmitted to the changeover switch and further to the different nodes through the classical channels. In the experiment, the gains of the amplitude quadrature g_X and phase quadrature g_Y are equal and unity to transfer the arbitrary quantum state[3,4] (see more details in the supplementary material). The classical outcomes communicated to AM_n and PM_n located in the AUX belong to node n, which perform a conditional displacement to reconstruct the input state.[14]

In each node n, the AUX carrying the acquired information is combined with the $\mathrm{EPR}_{-n\omega}$ at a 99:1 BS to reassemble the initial input state and accomplish the teleportation protocol. The output beam is verified with the measured BHD by interfering with the $\mathrm{LO}_{-n\omega}$. All the above-mentioned homemade BHDs with more than 50 MHz bandwidth (75 dB common mode rejection ratio) are utilized to ensure the accuracy and reliability of the results.[52] The alternating current (AC) output of BHD at node n is split into two parts via a power splitter. One is measured by a spectrum analyzer to obtain the noise power in the frequency domain. The other is mixed with an electrical signal of 3 MHz to get the time-domain signal with an oscilloscope to reconstruct the Wigner function of the teleported state.[42,43] Finally, we can calculate the fidelity from the noise power and the Wigner function of the output state to verify whether the quantum teleportation protocol is implemented.

Before teleportation process, we switch the settings of four nodes manually and measured the correlated noise powers between the four pairs of entangled sideband modes, as shown in Fig. 4(a). The correlation amplitude variances are measured of -7.3 ± 0.1 dB, -7.2 ± 0.1 dB, -6.9 ± 0.2 dB, and -6.9 ± 0.2 dB and phase variances are -7.2 ± 0.1 dB, -7.1 ± 0.1 dB, -7.0 ± 0.2 dB, and -6.8 ± 0.2 dB, respectively. Meanwhile, the entangled correlation parameters r can be

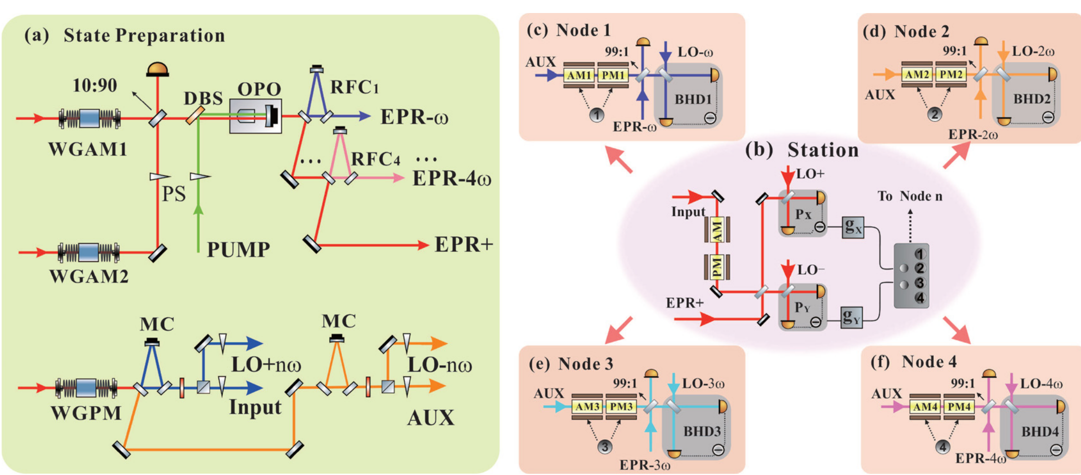

FIG. 3. Schematic of experimental setup for 4-branch quantum teleportation network with star topology. (a) State preparation. (b)–(f) Quantum teleportation protocol. WGAM, waveguide amplitude modulator; WGPM, waveguide phase modulator; DBS, dichroic beam splitter; OPO, optical parameter oscillator; PS, phase shifter; RFC, ring filter cavity; MC, mode cleaner; AM, amplitude modulator; PM, phase modulator; PD, photo detector; AUX, auxiliary beam; BHD, balanced homodyne detector; LO, local oscillator; g_X and g_Y, classical gain.

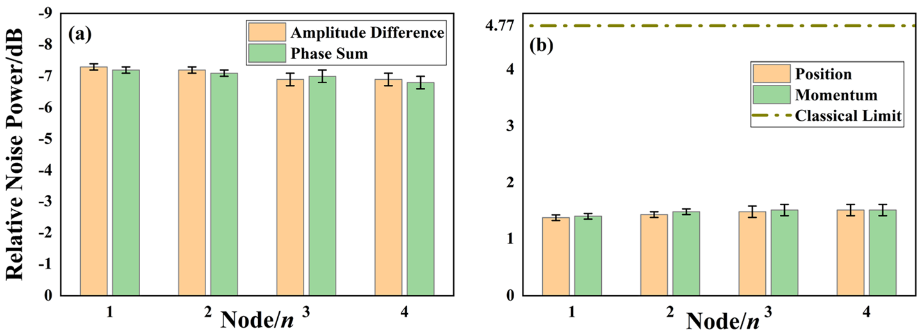

FIG. 4. (a) Relative spectral densities of four pairs of entangled sideband modes at node n ($n = 1$, 2, 3, 4), respectively. (b) Relative noise power spectras of the teleported states for the position and momentum measured recorded at node n ($n = 1$, 2, 3, 4), respectively. The error bars are obtained from the standard deviations of 20 times repeated measurements.

inferred. For amplitude quadrature, the correlation parameters are $r_{x1} = 0.841 \pm 0.011$, $r_{x2} = 0.829 \pm 0.012$, $r_{x3} = 0.795 \pm 0.023$, and $r_{x4} = 0.795 \pm 0.023$, respectively, and for phase quadrature, the correlation parameters are $r_{p1} = 0.829 \pm 0.012$, $r_{p2} = 0.818 \pm 0.011$, $r_{p3} = 0.806 \pm 0.023$, and $r_{p4} = 0.783 \pm 0.023$, respectively. The high-quality quantum entanglement provides the possibility for high-fidelity quantum teleportation. Figure 4(b) represents the results of each independent communication link in the quantum teleportation star network. The classical limit, dotted yellow line in Fig. 4(b), shows the noise power of the classical teleported state and is 4.77 dB higher than the shot noise limit (SNL) as expected.[14] The bar graphs above the SNL show the amplitude quadrature and phase quadrature noise powers of the quantum teleported states at node n ($n = 1$, 2, 3, 4) when the central station and nodes share the entangled sideband modes and the phase of LO is locked. All data are the noise variances recorded by node n with a vacuum state input at the analysis frequency of 3 MHz (see more details in the supplementary material).

In the presence of decoherence, the quality of the reconstructed state may be quantified by its teleported fidelity $F \equiv \langle a_{in}|\rho_{out}|a_{in}\rangle$, which represents the overlap extent between input state and output state, ρ_{out} is the density matrix of the output state.[14–16] The gain factor g of the classical channels is selected as unity value for amplitude and phase quadrature. In the experiment, the fidelity also can be written as $F = \frac{2}{\sqrt{(1+\sigma_W^x)(1+\sigma_W^p)}}$ for a Gaussian state,[54] where $\sigma_W^x = \sigma_W^p = g^2 + \frac{1}{2}e^{2r}(1-g)^2 + \frac{1}{2}e^{-2r}(1+g)^2$. σ_W^x and σ_W^p are the noise variances of amplitude and phase quadratures of the output state. The Wigner function is performed to describe the quasi-probability distribution of quadrature amplitude and phase and complete quantum state characteristics in phase space,[55,56] as shown in Fig. 5. All the illustrations are in the top view, which can intuitively benchmark the quality of the teleportation. Figure 5(a) is the reconstructed Wigner function of the initial input state $|a_{in}\rangle$ detected at each node. As shown in Fig. 5(b), the input state is directly measured and then the results are delivered to output to prepare the output state in the absence of entanglement, which represents the classical teleportation with the fidelity of $F_{class} = 0.5$. Based on the no-cloning theorem, the teleported state is the best remaining copy of the input state when the entanglement degree is 3 dB, whose fidelity is $F_{no-cloning} = 2/3$.[57,58] With the stronger quantum correlation, the fidelity can go beyond the classical limit of $F > F_{no-cloning}$. The fidelities of the reassembled state with the help of entangled sideband modes are $F_1 = 0.843 \pm 0.003$, $F_2 = 0.839 \pm 0.004$, $F_3 = 0.837 \pm 0.007$, and $F_4 = 0.830 \pm 0.007$ at node 1–4, as indicated in Figs. 5(c)–5(f). By utilizing the entangled correlation parameters r, the theoretical fidelities can be calculated. These results are in good agreement with the fidelities of the reassembled states. Therefore, we achieve a 4-branch quantum teleportation star network with all fidelities superior to the no-cloning limit.

In conclusion, we have proposed a 4-branch star-topology network to construct the CV quantum teleportation protocol exploiting

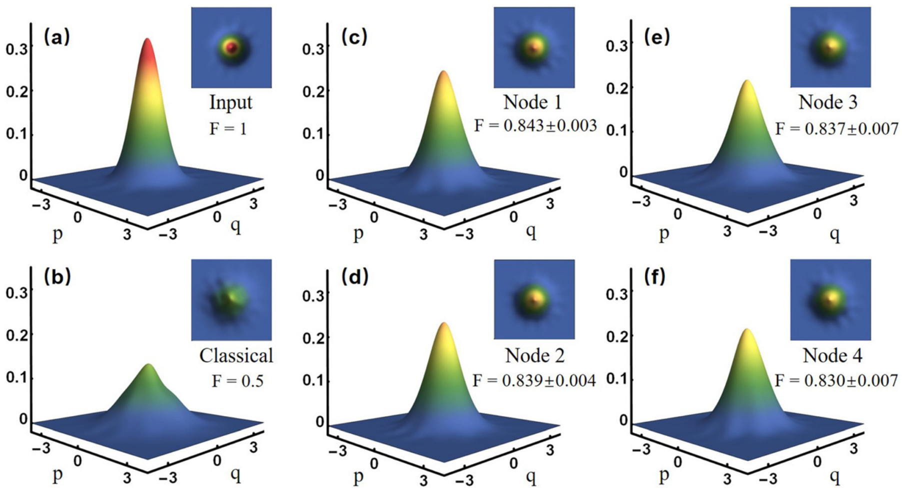

FIG. 5. Reconstructed Wigner functions. (a) Input state, (b) classical teleported state, and (c)–(f) quantum teleported states at node n ($n = 1$, 2, 3, 4). The p and q are momentum and position in the phase space, respectively.

the multiplex entangled sideband modes. Thanks to the innovative generation scheme of the FCSB, we implement four pairs of entangled sideband modes by directly injecting the FCSB into OPO, which effectively simplifies the experimental setup and reduces the additional loss as far as possible. By employing four cascade RFCs, the entangled sideband modes are distributed to central station and other nodes. Subsequently, the quantum teleportation network is implemented within several users, and the fidelities of the reconstructed output states at each node are 0.843 ± 0.003, 0.839 ± 0.004, 0.837 ± 0.007, and 0.830 ± 0.007, respectively, which are superior to the no-cloning limit 2/3. With the advanced material technology, such as the advance of WGAM and silicon-based elements,[59,60] we expect to extend the present system to more nodes, and we believe that the star-topology quantum communication network with more branches will have a bright future. This demonstration of a quantum teleportation network with a star topology may further enrich the toolbox of star topology networks and provide more possibilities for constructing complex topologies that combine multiple simple architectures with continuous variables.[61]

See the supplementary material for the (1) analysis of the error signal for squeezing angle manipulation, (2) experiment setup, (3) method of calibrating the teleportation gain factors, and (4) experiment results.

This work was supported by the National Natural Science Foundation of China (NSFC) (Grant Nos. 62225504, 62027821, U22A6003, 12174234, 62375162, and 12304399) and the Fundamental Research Program of Shanxi Province (Nos. 202303021212003 and 202303021224006).

AUTHOR DECLARATIONS

Conflict of Interest

The authors have no conflicts to disclose.

Author Contributions

Yimiao Wu and Long Tian contributed equally to this work.

Yimiao Wu: Data curation (lead); Investigation (lead); Writing – original draft (equal); Writing – review & editing (equal). **Long Tian:** Formal analysis (lead); Funding acquisition (equal); Supervision (lead). **Wenxiu Yao:** Investigation (equal). **Shaoping Shi:** Conceptualization (lead); Validation (lead); Writing – original draft (equal). **Xuan Liu:** Data curation (equal). **Bo Lu:** Data curation (equal). **Yajun Wang:** Data curation (equal); Funding acquisition (equal); Supervision (equal). **Yaohui Zheng:** Funding acquisition (lead); Methodology (lead); Project administration (lead); Resources (lead); Writing – review & editing (lead).

DATA AVAILABILITY

The data that support the findings of this study are available from the corresponding authors upon reasonable request.

REFERENCES

[1] C. H. Bennett, G. Brassard, C. Crépeau, R. Jozsa, A. Peres, and W. K. Wootters, "Teleporting an unknown quantum state via dual classical and Einstein-Podolsky-Rosen channels," Phys. Rev. Lett. **70**, 1895–1899 (1993).

[2] D. Bouwmeester, J.-W. Pan, K. Mattle, M. Eibl, H. Weinfurter, and A. Zeilinger, "Experimental quantum teleportation," Nature **390**, 575–579 (1997).

[3] A. Furusawa, J. L. Sørensen, S. L. Braunstein, C. A. Fuchs, H. J. Kimble, and E. S. Polzik, "Unconditional quantum teleportation," Science **282**, 706–709 (1998).

[4] S. Pirandola, J. Eisert, C. Weedbrook, A. Furusawa, and S. L. Braunstein, "Advances in quantum teleportation," Nat. Photonics **9**, 641–652 (2015).

[5] K. Mattle, H. Weinfurter, P. G. Kwiat, and A. Zeilinger, "Dense coding in experimental quantum communication," Phys. Rev. Lett. **76**, 4656–4659 (1996).

[6] S. L. Braunstein and H. J. Kimble, "Dense coding for continuous variables," Phys. Rev. A **61**, 042302 (2000).

[7] S. L. Braunstein and P. van Loock, "Quantum information with continuous variables," Rev. Mod. Phys. **77**, 513–577 (2005).

[8] F. Grosshans, G. V. Assche, J. Wenger, R. Brouri, N. J. Cerf, and P. Grangier, "Quantum key distribution using Gaussian-modulated coherent states," Nature **421**, 238–241 (2003).

[9] H.-K. Lo, M. Curty, and B. Qi, "Measurement-device-independent quantum key distribution," Phys. Rev. Lett. **108**, 130503 (2012).

[10] H.-K. Lo, M. Curty, and K. Tamaki, "Secure quantum key distribution," Nat. Photonics **8**, 595–604 (2014).

[11] M. Hillery, V. Bužek, and A. Berthiaume, "Quantum secret sharing," Phys. Rev. A **59**, 1829–1834 (1999).

[12] R. Ursin and R. Hughes, "Sharing quantum secrets," Nature **501**, 37–38 (2013).

[13] D. Gottesman, "Theory of quantum secret sharing," Phys. Rev. A **61**, 042311 (2000).

[14] X. Wang, X. Cai, Z. Su, M. Chen, D. Wu, L. Li, N. Liu, C. Lu, and J. Pan, "Quantum teleportation of multiple degrees of freedom in a single photon," Nature **518**, 516–519 (2015).

[15] N. Takei, T. Aoki, S. Koike, K.-I. Yoshino, K. Wakui, H. Yonezawa, T. Hiraoka, J. Mizuno, M. Takeoka, M. Ban, and A. Furusawa, "Experimental demonstration of quantum teleportation of a squeezed state," Phys. Rev. A **72**, 042304 (2005).

[16] N. Lee, H. Benichi, Y. Takeno, S. Takeda, J. Webb, E. Huntington, and A. Furusawa, "Teleportation of nonclassical wave packets of light," Science **332**, 330–333 (2011).

[17] X. Su, C. Tian, X. Deng, Q. Li, C. Xie, and K. Peng, "Quantum entanglement swapping between two multipartite entangled states," Phys. Rev. Lett. **117**, 240503 (2016).

[18] S. Liu, Y. Lou, and J. Jing, "Orbital angular momentum multiplexed deterministic all-optical quantum teleportation," Nat. Commun. **11**, 3857 (2020).

[19] S. Takeda, T. Mizuta, M. Fuwa, P. van Loock, and A. Furusawa, "Deterministic quantum teleportation of photonic quantum bits by a hybrid technique," Nature **500**, 315–318 (2013).

[20] K. Zhang, S. Liu, Y. Chen, X. Wang, and J. Jing, "Optical quantum states based on hot atomic ensembles and their applications," Photonics Insights **1**, R06 (2022).

[21] N. Takei, H. Yonezawa, T. Aoki, and A. Furusawa, "High-fidelity teleportation beyond the no-cloning limit and entanglement swapping for continuous variables," Phys. Rev. Lett. **94**, 220502 (2005).

[22] H.-J. Briegel, W. Dür, J. I. Cirac, and P. Zoller, "Quantum repeaters: The role of imperfect local operations in quantum communication," Phys. Rev. Lett. **81**, 5932–5935 (1998).

[23] J.-L. Wu, Y. Wang, J.-X. Han, Y.-K. Feng, S.-L. Su, Y. Xia, Y. Jiang, and J. Song, "One-step implementation of Rydberg-antiblockade swap and controlled-swap gates with modified robustness," Photonics Res. **9**, 814–821 (2021).

[24] E. Knill, R. Laflamme, and G. J. Milburn, "A scheme for efficient quantum computation with linear optics," Nature **409**, 46–52 (2001).

[25] L. S. Madsen, F. Laudenbach, M. F. Askarani, F. Rortais, T. Vincent, J. F. F. Bulmer, F. M. Miatto, L. Neuhaus, L. G. Helt, M. J. Collins, A. E. Lita, T. Gerrits, S. W. Nam, V. D. Vaidya, M. Menotti, I. Dhand, Z. Vernon, N. Quesada, and J. Lavoie, "Quantum computational advantage with a programmable photonic processor," Nature **606**, 75–81 (2022).

[26] W. Asavanant, Y. Shiozawa, S. Yokoyama, B. Charoensombutamon, H. Emura, R. N. Alexander, S. Takeda, J.-I. Yoshikawa, N. C. Menicucci, H. Yonezawa, and A. Furusawa, "Generation of time-domain-multiplexed two-dimensional cluster state," Science **366**, 373–376 (2019).

[27] Q. Wang, Y. Tian, W. Li, L. Tian, Y. Wang, and Y. Zheng, "High-fidelity quantum teleportation toward cubic phase gates beyond the no-cloning limit," Phys. Rev. A **103**, 062421 (2021).
[28] B. Fröhlich, J. F. Dynes, M. Lucamarini, A. W. Sharpe, Z. Yuan, and A. J. Shields, "A quantum access network," Nature **501**, 69–72 (2013).
[29] H. J. Kimble, "The quantum internet," Nature **453**, 1023–1030 (2008).
[30] F. Centrone, F. Grosshans, and V. Parigi, "Cost and routing of continuous-variable quantum networks," Phys. Rev. A **108**, 042615 (2023).
[31] W. Wang, K. Zhang, and J. Jing, "Large-scale quantum network over 66 orbital angular momentum optical modes," Phys. Rev. Lett. **125**, 140501 (2020).
[32] N.-N. Wang, A. Pozas-Kerstjens, C. Zhang, B.-H. Liu, Y.-F. Huang, C.-F. Li, G.-C. Guo, N. Gisin, and A. Tavakoli, "Certification of non-classicality in all links of a photonic star network without assuming quantum mechanics," Nat. Commun. **14**, 2153 (2023).
[33] Y. Ren, X. Wang, Y. Lv, D. Bacco, and J. Jing, "Distribution of multiplexed continuous-variable entanglement for quantum networks," Laser Photonics Rev. **16**, 2100586 (2022).
[34] K. Wei, W. Li, H. Tan, Y. Li, H. Min, W.-J. Zhang, H. Li, L. You, Z. Wang, X. Jiang, T.-Y. Chen, S.-K. Liao, C.-Z. Peng, F. Xu, and J.-W. Pan, "High-speed measurement-device-independent quantum key distribution with integrated silicon photonics," Phys. Rev. X **10**, 031030 (2020).
[35] D. Poderini, I. Agresti, G. Marchese, E. Polino, T. Giordani, A. Suprano, M. Valeri, G. Milani, N. Spagnolo, G. Carvacho, R. Chaves, and F. Sciarrino, "Experimental violation of n-locality in a star quantum network," Nat. Commun. **11**, 2467 (2020).
[36] S. Wengerowsky, S. K. Joshi, F. Steinlechner, H. Hübel, and R. Ursin, "An entanglement-based wavelength-multiplexed quantum communication network," Nature **564**, 225–228 (2018).
[37] S. K. Joshi, D. Aktas, S. Wengerowsky, M. Lončarić, S. P. Neumann, B. Liu, T. Scheidl, G. C. Lorenzo, Ž. Samec, L. Kling, A. Qiu, M. Razavi, M. Stipčević, J. G. Rarity, and R. Ursin, "A trusted node-free eight-user metropolitan quantum communication network," Sci. Adv. **6**, eaba0959 (2020).
[38] M. Cuquet and J. Calsamiglia, "Entanglement percolation in quantum complex networks," Phys. Rev. Lett. **103**, 240503 (2009).
[39] J. Miguel-Ramiro, F. Riera-Sàbat, and W. Dür, "Quantum repeater for *W* states," PRX Quantum **4**, 040323 (2023).
[40] B.-S. Shi and A. Tomita, "Teleportation of an unknown state by *W* state," Phys. Lett. A **296**, 161–164 (2002).
[41] M. Sasaki, M. Fujiwara, H. Ishizuka *et al.*, "Field test of quantum key distribution in the Tokyo QKD Network," Opt. Express **19**, 10387–10409 (2011).
[42] A. Cavaillès, H. Le Jeannic, J. Raskop, G. Guccione, D. Markham, E. Diamanti, M. D. Shaw, V. B. Verma, S. W. Nam, and J. Laurat, "Demonstration of Einstein-Podolsky-Rosen steering using hybrid continuous- and discrete-variable entanglement of light," Phys. Rev. Lett. **121**, 170403 (2018).
[43] N. H. Nickerson, Y. Li, and S. C. Benjamin, "Topological quantum computing with a very noisy network and local error rates approaching one percent," Nat. Commun. **4**, 1756 (2013).
[44] S. L. N. Hermans, M. Pompili, H. K. C. Beukers, S. Baier, J. Borregaard, and R. Hanson, "Qubit teleportation between non-neighbouring nodes in a quantum network," Nature **605**, 663–668 (2022).
[45] S. Shi, Y. Wang, L. Tian, J. Wang, X. Sun, and Y. Zheng, "Observation of a comb of squeezed states with a strong squeezing factor by a bichromatic local oscillator," Opt. Lett. **45**, 2419–2422 (2020).
[46] J. Zhang, "Einstein-Podolsky-Rosen sideband entanglement in broadband squeezed light," Phys. Rev. A **67**, 054302 (2003).
[47] M. Pysher, Y. Miwa, R. Shahrokhshahi, R. Bloomer, and O. Pfister, "Parallel generation of quadripartite cluster entanglement in the optical frequency comb," Phys. Rev. Lett. **107**, 030505 (2011).
[48] J. Roslund, R. M. de Araújo, C. F. S. Jiang, and N. Treps, "Wavelength-multiplexed quantum networks with ultrafast frequency combs," Nat. Photonics **8**, 109–112 (2014).
[49] S. Shi, L. Tian, Y. Wang, Y. Zheng, C. Xie, and K. Peng, "Demonstration of channel multiplexing quantum communication exploiting entangled sideband modes," Phys. Rev. Lett. **125**, 070502 (2020).
[50] L. Tian, S. Shi, Y. Li, Y. Wu, W. Li, Y. Wang, Q. Liu, and Y. Zheng, "Entangled sideband control scheme via frequency-comb-type seed beam," Opt. Lett. **46**, 3989–3992 (2021).
[51] Y. Wu, Q. Wang, L. Tian, X. Zhang, J. Wang, S. Shi, Y. Wang, and Y. Zheng, "Multi-channel multiplexing quantum teleportation based on the entangled sideband modes," Photonics Res. **10**, 1909–1914 (2022).
[52] T. Eberle, V. Händchen, and R. Schnabel, "Stable control of 10 dB two-mode squeezed vacuum states of light," Opt. Express **21**, 11546–11553 (2013).
[53] H. Vahlbruch, M. Mehmet, K. Danzmann, and R. Schnabel, "Detection of 15 dB squeezed states of light and their application for the absolute calibration of photoelectric quantum efficiency," Phys. Rev. Lett. **117**, 110801 (2016).
[54] B. Schumacher, "Sending entanglement through noisy quantum channels," Phys. Rev. A **54**, 2614–2628 (1996).
[55] P. Barriga, C. Zhao, and D. G. Blair, "Optical design of a high power mode-cleaner for AIGO," Gen. Relativ. Gravitation **37**, 1609–1619 (2005).
[56] E. H. Huntington and T. C. Ralph, "Separating the quantum sidebands of an optical field," J. Opt. B: Quantum Semiclassical Opt. **4**, 123 (2002).
[57] F. Grosshans and P. Grangier, "Quantum cloning and teleportation criteria for continuous quantum variables," Phys. Rev. A **64**, 010301 (2001).
[58] T. C. Zhang, K. W. Goh, C. W. Chou, P. Lodahl, and H. J. Kimble, "Quantum teleportation of light beams," Phys. Rev. A **67**, 033802 (2003).
[59] J. S. Levy, A. Gondarenko, M. A. Foster, A. C. Turner-Foster, A. L. Gaeta, and M. Lipson, "CMOS-compatible multiple-wavelength oscillator for on-chip optical interconnects," Nat. Photonics **4**, 37–40 (2010).
[60] G. Masada, K. Miyata, A. Politi, T. Hashimoto, J. L. O'Brien, and A. Furusawa, "Continuous-variable entanglement on a chip," Nat. Photonics **9**, 316–319 (2015).
[61] X.-M. Hu, Y. Guo, B.-H. Liu, C.-F. Li, and G.-C. Guo, "Progress in quantum teleportation," Nat. Rev. Phys. **5**, 339–353 (2023).